We are IntechOpen, the world's leading publisher of Open Access books Built by scientists, for scientists

4,800
Open access books available

122,000
International authors and editors

135M
Downloads

Our authors are among the

154
Countries delivered to

TOP 1%
most cited scientists

12.2%
Contributors from top 500 universities

CLARIVATE ANALYTICS BOOK CITATION INDEX INDEXED

WEB OF SCIENCE™

Selection of our books indexed in the Book Citation Index in Web of Science™ Core Collection (BKCI)

Interested in publishing with us?
Contact book.department@intechopen.com

Numbers displayed above are based on latest data collected.
For more information visit www.intechopen.com

17

Ant Colony Optimization for Image Segmentation

Yuanjing Feng and Zhejin Wang
Zhejiang University of Technology
China

1. Introduction

Image segmentation is a complex visual computation problem, which refers to the process of distinguishing objects from background. Ant colony optimization (ACO) is a cooperative search algorithm inspired by the behavior of real ants. In order to achieve an approving performance, we use ACO global optimization algorithm to solve image segmentation problems.

1.1 Related literature

A variety of approaches have been developed for solving image segmentation problems. In these approaches, different methods have defined various cost functions for the task of image segmentation. A popular tool for minimization of these cost functions is the curve evolution framework and active contour model (ACM). ACMs have been proposed by Kass et al. (1987) which converts the segmentation to a functional extremum problem. Within ACM framework, evolution of the curves can be controlled by segmentation cost functions, external force fields, and geometric forces such as curvature flow and constant expansion forces (e.g., balloons, see Cohen, 1991). Many approaches have been proposed to solve this model, such as, greedy algorithm, dynamic programming method, directional image force method, genetic algorithm(GA) snakes method and so on (Amini et al., 1990; Williams & Shah, 1990; MacEachern & Manku, 1998; Gunn & Nixon, 1996; Xu & Prince, 1998; Hsien-Hsun et al., 2000; Lam & Yan, 1994; Mishraa et al., 2003). However, these methods still cannot perform very well. For example, the greedy algorithm has a high efficiency, but it cannot guarantee the global convergence (Lam & Yan, 1994). GA and SA are proved to be convergent with probability one, nonetheless the procedure is time-consuming (Mishraa et al., 2003).

ACO is first introduced by M. Dorigo (Dorigo et al., 1996). One basic idea of the ACO approach is to use the counterpart of the pheromone trail used by real ants as a medium for communication and as an indirect form of memory of previously found solutions. The artificial ants are simple agents that have some basic capabilities, e.g., the case of the traveling salesman problem (TSP). They may use some heuristic information like the distance between cities to construct tours and maintain a tabu list in which they store the partial tour constructed so far. The ants build solutions constructively guided by heuristic information and the pheromone trails left by ants in previous iterations. ACO has been applied successfully to numerous combinatorial optimization problems including in TSP (Dorigo & Ganbardella, 1997), vehicle routing problem (Bullnheimer et al., 1998), flow shop

problem (Stutzle, 1998) and others. The successful applications of ACO attract image processing researchers' attention. Quadfel et al. proposed an algorithm for image segmentation based on the Markov Random Field (MRF) and ACO (Ouadfel & Batouche, 2003). S.Meshoul cast the point matching problem in point-based image registration method as combinatorial optimization task and solved by ACO (Meshoul & Batouche, 2003). In our previous work, an ACO algorithm similar to MAX-MIN ant system for image segmentation based on ACM was developed (Feng, 2005). This method is usually more effective than the other global optimization algorithms such as GA and SA.

In recent years, more and more novel ACO algorithms are advanced by researchers. An improved ACO for fuzzy clustering in image segmentation has been proposed by Han et al.(Han & Shi, 2006). In their paper, three features such as gray value, gradient and neighborhood of the pixels, are extracted for the searching and clustering process. They make improvements by initializing the clustering centers and enhancing the heuristic function to accelerate the searching process. Tests show ACO is successfully applied in image segmentation combined with fuzzy clustering. Then, Tao et al. present an object segmentation method using ACO algorithm and fuzzy entropy (Tao et al., 2007). They have investigated the infrared object segmentation performance of the fuzzy entropy principle and additionally, designed an ACO strategy to find the optimal combination of all the parameters.

Moreover, a new approach that concerns ACO for image regularization based on a nonstationary markov modelling was proposed by Le Hegarat-Mascle et al. (Hegarat-Mascle et al., 2007). They show that this corresponds to an automatic adaptation of the neighborhood to the segment form, and that it outperforms the fixed-form neighborhood used in classical Markov random field regularization techniques. The performance of this new approach is illustrated on a simulated image and on actual remote sensing images. Two years later, Ma et al. put forward a universal texture segmentation and representation scheme based on ACO for iris image processing (Ma et al, 2009). They propose a framework for ACO based image processing methods and create the flexibility of defining different mechanisms for an ant's behaviour according to various problems, which turned out competitive and quite promising, with excellent effectiveness and practicability especially for images with complex local texture situations. Besides, in terms of the pheromone, someone has proposed a new algorithm for image segmentation based on the concept of aggregation pheromone density, which is inspired by the ants' property to accumulate around points with higher pheromone density (Susmita et al., 2009).

1.2 Contributions

This chapter introduces two ant colony algorithms for image segmentation in ACM framework. We first present a new ant colony algorithm based on boundary searching process of ACM, which uses ACO to search for the best path in a constrained region. We describe how the image edge detection problem can be transferred to the ant colony searching process by means of constructing cost function, solution space, pheromone model, and heuristic information. However, the previous work of ACO on ACM shows that this algorithm is also time-consuming. One of the main causes is the updating method of the pheromone in general ACO. Experimental results show general ACO algorithms try to update the pheromone values in such a way that the probability to generate high-quality solutions increases over time. Second, in consideration of the computation burden, a modified ACO called finite grade ACO (FGACO) is proposed. It classifies pheromone into finite grades, the higher the grade, the more the pheromone. Moreover, updating of the

pheromone is achieved by changing the grades. The updated quantity of pheromone is independent from the objective function, and the grade is changed by addition and subtraction operations. The algorithm is proved to converge to the global optimal solutions linearly by means of finite Markov chains. Finally, the proposed algorithm is applied in phase change line detection of complex phase change thermography. In this part we apply ACM based ACO algorithm to sub-image segmentation, which converts image segmentation to a problem of searching for the best path in a constrained region. The experimental results show that the algorithm extracts the phase change active contour well.

2. Ant colony optimization for active contour model based image segmentation

2.1 Active contour model in image segmentation

As formulated above, ACM is a popular tool for the minimization of cost functions. The original ACM described by Kass et al. (1987) refers to a set of points, $v(s) = (x(s), y(s))$, on an image parameterized with respect to the contour length, s. Each possible configuration of the contour has an energy associated with it, which is a combination of internal and external energies. The energy function can be written as:

$$E_{snake} = \int_0^1 E_{snake}(v(s))ds = \int_0^1 [E_{\text{in}}(v(s)) + E_{image}(v(s)) + E_{con}(v(s))]ds \tag{1}$$

where E_{in} represents the internal energy of the active contour, E_{image} represents the image forces, and E_{con} represents the external constraint forces. The internal energy is composed of a first order and a second order term forcing the active contour to act like a membrane of a thin plate.

$$E_{\text{in}} = (\alpha(s)|v_s(s)|^2 + \beta(s)|v_{ss}(s)|^2) / 2 \tag{2}$$

Let $E_{ext} = E_{image} + E_{con}$, with

$$E_{image} = w_{line}E_{line} + w_{edge}E_{edge} + w_{cur}E_{cur} \tag{3}$$

The energy term due to image forces is a linear combination of line, edge and termination energy terms, all computed from an image, $I(x,y)$. $E_{line} = I(x,y)$, $E_{edge} = -|\nabla I(x,y)|^2$ and E_{cur} is the curvature of the level contours in a Gaussian smoothed image.
The energy integral becomes

$$\int_0^1 E_{ext}(v(s)) + \frac{1}{2}(\alpha(s)|v_s(s)|^2 + \beta(s)|v_{ss}(s)|^2)ds \tag{4}$$

According to the lemma of necessary condition for functional extremum (Lao, 2004) to minimize (4), a pair of independent Euler equations is obtained (Amini & Jain, 1990),

$$-\alpha x_{ss} + \beta x_{ssss} + \frac{\partial E_{ext}}{\partial x} = 0 \tag{5}$$

$$-\alpha y_{ss} + \beta y_{ssss} + \frac{\partial E_{ext}}{\partial y} = 0 \tag{6}$$

Discretizing the above equation with $f_x(i) = \frac{\partial E_{ext}}{\partial x_i}$ and $f_y(i) = \frac{\partial E_{ext}}{\partial y_i}$, we get

$$\begin{aligned}\alpha_i(v_i - v_{i-1}) - \alpha_{i+1}(v_{i+1} - v_i) + \beta_{i-1}(v_{i-2} - 2v_{i-1} + v_i) \\ -2\beta_i(v_{i-1} - 2v_i + v_{i+1}) + \beta_{i+1}(v_i - 2v_{i+1} + v_{i+2}) + (f_x(i), f_y(i)) = 0\end{aligned} \tag{7}$$

with $v(0) = v(n)$ .Writing (7) in matrix forms, it has

$$Ax + f_x(x, y) = 0 \tag{8}$$

$$Ay + f_y(x, y) = 0 \tag{9}$$

Discretizing the energy term in (2), it has the form

$$\begin{aligned}E_{snake} &= \sum_{i=0}^{n-1} E_{\text{int}}(i) + E_{ext}(i) \\ &= \sum_{i=0}^{n-1} E_{\text{int}}(i) + E_{ext}(i) \sum_{i=0}^{n-1} (\alpha_i \left| v_i - v_{i-1} \right|^2 + \beta_i \left| v_{i-1} - 2v_i + v_{i+1} \right|^2) / 2 + E_{ext}(i)\end{aligned} \tag{10}$$

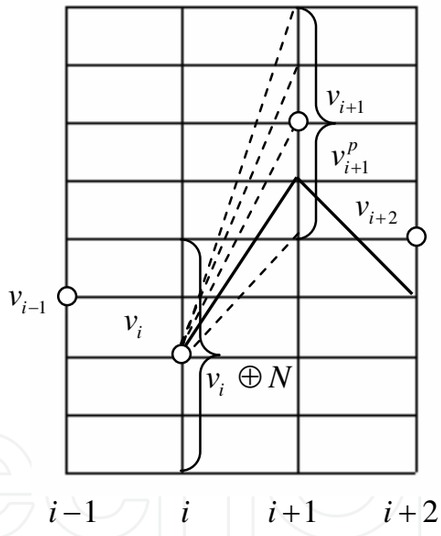

Fig. 1. Searching graph

The problem of energy minimization can be viewed as a discrete multistage decision process. At each stage, only a local neighborhood of a point on the active contour is considered. This characterizes the set of admissible paths in each iteration. For convenience, let us first consider only the first order term of the internal energy measure. With i representing the stage and k the possible choices at each stage, the multistage decision problem of (10) can be computed to be:

$$E_t(i+1, k) = E_t(i, k) + \frac{1}{2}\alpha_i(v_{i+1} \oplus k - v_i \oplus j)^2 + E_{ext}(v_{i+1} \oplus k) \tag{11}$$

where, $0 \le k \le N$ (N being the number of possible directions at each stage), v_m is the m^{th} point on the active contour, and $\oplus$ is an operation by which all the points in a local neighborhood of a given point on the lattice are generated.

The image can be represented as the grid shown in Fig.1. The connection of nodes $\{v_1, v_2, \cdots, v_n\}$, is the initial contour. Supposing that $v_i^l \in v_i \oplus N$ is the current edge point, then the next point is the choice point or not depends on whether it makes the energy function (10) decrease.

Let us now consider the case where the second order term is also included in the internal energy measure. When including this in the computation of $E_{\min}(t)$, at stage $i+1$ one should consider all the possible points at stage i. However, it would be a pitfall to consider only the (i,k) entry of the position matrix for the point at stage $i-1$. We need to consider all the possible combinations for the i and $i-1$ stages once at stage $i+1$.

The energy for each sub-cell is computed to be:

$$\begin{aligned} E_t(i+1,j,k) = E_t(i,k,m) + E_{ext}(v_i \oplus k) + \frac{1}{2}\alpha_i(v_i \oplus k - v_{i-1} \oplus m)^2 \\ + \beta_i(v_{i+1} \oplus j - 2v_i \oplus k + v_{i-1} \oplus m)^2 \end{aligned} \tag{12}$$

2.2 Graph based ant colony optimization

Consider a minimization problem (S, f, Ω) where S is the set of (candidate) solutions, f is the objective function, which assigns to each candidate solution max(•) an objective function (cost) value $f(s)$, and Ω is a set of constraints, which defines the set of feasible candidate solutions. The goal of the minimization (S, f, Ω) problem is to find an optimal solution, i.e., a feasible candidate solution of minimum cost. The combinatorial optimization problem (S, f, Ω) is mapped on a problem that can be characterized by the following.

1. A finite set $\varsigma = \{c_1, c_2, \cdots, c_{NC}\}$ of components.
2. A finite set χ of states of the problem, defined in terms of all possible sequences $x = < c_i, c_j, \cdots, c_k, \cdots >$ over the elements of ς.
3. The set of (candidate) solutions S is a subset of χ (i.e., $S \subseteq \chi$).
4. A set of feasible states $\tilde{\chi}$, with $\tilde{\chi} \subseteq \chi$, defined via a problem-dependent test that verifies that it is not impossible to complete a sequence $x \in \tilde{\chi}$ into a solution satisfying the constraints Ω.
5. A nonempty set S^* of optimal solutions, with $S^* \subseteq \tilde{\chi}$ and $S^* \subseteq S$.

In the given above formulation, the combinatorial optimization problem (S, f, Ω) can be expressed as the graph $G = (\varsigma, \Lambda)$ called construction graph, where the vertices are the components ς, the set Λ fully connects the components ς. The vector $\tau(n)$ is pheromone values on the arcs of ς at iteration n, and the vector $\hat{s}(n)$ is the current optimal path at iteration n with corresponding cost function values $\hat{f}(n)$.

In the ACO algorithm, ants start from an initial node, perform repetitive stochastic transitions form one node to another node and find feasible routes that correspond to the feasible solutions of the optimization problem. The optimization process can be represented as:

1. Ant solution construction

While ($H(\bullet)$ and $x_k \notin S$) do:

At each step k after building the sequence $x_k =< c_1, c_2, \cdots, c_k >$, select the next vertex l randomly following

$$p_{kl} = \begin{cases} \dfrac{(\tau_{kl})^{\alpha}(\eta_{kl})^{\beta}}{\sum_{(c_k, y)\in J_{ck}} (\tau_{ky})^{\alpha}(\eta_{kl})^{\beta}} & if (c_k, c) \in J_{ck} \\ 0 & otherwise \end{cases} \tag{13}$$

where η_{kl} is heuristic information value corresponding to the cost function. α, β are the weight parameters respectively for pheromone and heuristic information value in p_{kl}. And a connection $(c_k, y) \in J_{ck}$ if the sequence $x_{k+1} =< c_1, c_2, \cdots, c_k, y >$ is such that $x_{k+1} \in \tilde{\chi}$. If J_{ck} is empty, the solution construction is finished.

2. Pheromone update

Once all the ants have terminated their local searches, a pheromone update phase is started in which pheromone trails are modified. Let $\hat{s}$ be the best feasible solution found so far and s_t be the best feasible solution in the current algorithm iteration t; $f(\hat{s})$ and $f(s_t)$ are the corresponding objective function values. The pheromone update procedure decreases by a small factor ρ, called the evaporation rate, the value of the pheromone trails on all the connections in Λ and then increases the value of the pheromone trails on the connections belonging to $\hat{s}$. The pheromone update procedure is described as follows.

(u1) $\forall (i, j): \tau_{ij} \leftarrow (1-\rho) \cdot \tau_{ij}$

(u2) if $f(s_t) < f(\hat{s})$, then $\hat{s} \leftarrow s_t$

(u3) $\forall (i, j) \in \hat{s}: \tau_{ij} \leftarrow \tau_{ij} + \rho \cdot g(\hat{s})$

(u4) $\forall (i, j): \tau_{ij} \leftarrow \max\{\tau_{\min}, \tau_{ij}\}$ (14)

where $0 < \rho < 1$ is the evaporation rate, $\tau_{\min} > 0$ is a parameter, and $g(s)$ is a function of s with: $f(s) < f(s') \Rightarrow g(s) \geq g(s')$.

2.3 Algorithm ingredients

To apply the ACO algorithm to the ACM based image segmentation problems, we must convert the ACM solving process to the searching graph. From the describing of above sections, the ACO can also be illustrated under the guidance of Fig.1. Supposing that theoretical contour has the minimal energy. Set an ant at $v_i^j \in v_i \oplus N$, it selects the next point $v_{i+1}^p \in v_{i+1} \oplus N$ under the influence of pheromone. With the cooperation of the ant colony, the path of final minimal energy is acquired.

Therefore, the solving process of ACM is quite similar to ACO. On the basis of our previous research (Feng, 2005), a kind of ACO that used to solve ACM is proposed, which provides a new efficient way for image segmentation.

2.3.1 Definition of pheromone

Set the ant at any position $v_i^j \in v_i \oplus N$ (there exists N choices), it will select any element from set $v_{i+1} \oplus N$ (there also exists N choices). That is, there are $N * N$ compages between the

two sets. If the contour is discretized into M points then the pheromone matrix τ_{ijk} is obtained, which consists of all adjacent connections. Where $i=(1,2,...M)$, $j,k=(1,2,...N)$.

2.3.2 Probability decision

Set the ant at the position of $v_i^j \in v_i \oplus N$, and the ant selects the next node $v_{i+1}^p \in v_{i+1} \oplus N$ according to the following probability,

$$\mathrm{P}\left(v_{i+1}^p \in v_{i+1} \oplus N \,\middle|\, v_i^j \in v_i \oplus N, \tau\right) = \begin{cases} \dfrac{\tau(i, v_i^j, v_{i+1}^p)^\alpha \cdot \eta(v_{i+1}^p)^\beta}{\sum_{l \in v_{i+1} \oplus N} \tau(i, v_i^j, v_{i+1}^l)^\alpha \cdot \eta(v_{i+1}^l)^\beta}, & l \in v_{i+1} \oplus N \\ 0, & others \end{cases} \tag{15}$$

where $i=(1,2,...M)$, $j,k=(1,2,...N)$, α,β are the weight parameters for pheromone and heuristic information value, respectively. $\tau(i, v_i^j, v_i^p)$ is the pheromone value on the arc (i, v_i^j, v_i^p). $\eta(v_{i+1}^p)$ is the heuristic information represented as

$$\eta(v_{i+1}^p) = 1 / [f(\nabla I)_{v_{i+1}^p}] \tag{16}$$

2.3.3 Pheromone update

(u5) $\forall(i,j,k)$: $\tau_{ijk} \leftarrow (1-\rho)\cdot\tau_{ijk}$

(u6) If $E_{snake}(t_{ai}) < E_{snake}(\hat{t}_{ai})$, then $t_{ai} \leftarrow \hat{t}_{ai}$

(u7) $\forall(i,j,k) \in \hat{t}$, $\tau_{ijk} \leftarrow \tau_{ijk} + \rho \cdot g(\hat{t})$ (17)

where $0<\rho<1$ is the evaporation rate, $g(t)$ is the function of path t, which satisfies: $E_{snake}(t) < E_{snake}(\hat{t}) \Rightarrow g(t) \geq g(\hat{t})$.

2.3.4 Solving process

The algorithm is described as follows：

Step 1. Given: Initial value $\forall(i,j,k)$, $\tau_{ijk}=\tau_0$, $\tau_0 \geq 0$; path t (decided by the initial contour).

Step 2. Calculate: For each dimension of search space, for each ant, select the next position v_{i+1}^p according to equation (15), until it satisfies the termination-criterion.

Step 3. Calculate: Energy E_{snake} of every path the ant passed, according to equation (10).

Step 4. Calculate: The minimized energy path $\hat{t}$ and update τ according to equation ((u5)~(u7)).

Step 5. Restoring: $\hat{t}$ is the best path of search space, so the best segmentation is obtained.

3. Finite grade pheromone ant colony optimization for image segmentation

3.1 Finite grade pheromone ant colony optimization

For the multistage decision of ACM based image segmentation problems, whose feasible decision set at each stage increases exponentially with the dimension of the decision variable. The previous work of ACO on ACM shows that the algorithm is also time-consuming. One of the main reasons is the updating method of the pheromone in general

ACO. From Eqs. (15) and (17), at run-time, ACO algorithms try to update the pheromone values in such a way that the probability to generate high-quality solutions increases over time. The pheromone values are updated using previously generated solutions. The update aims to concentrate the search in regions of the search space containing high-quality solutions. In particular, the reinforcement of solution components depending on the solution quality is an important ingredient of ACO algorithms. It implicitly assumes that good solutions consist of good solution components. To learn which components contribute to good solutions can help to assemble them into better solutions. Based on the experimental observation, during the run time of standard ACO, there are many arcs which have similar pheromone, and similar pheromone has almost the same effect on solution construction, this inspires us to classify pheromone into finite grades, and this motivates the FGACO for image segmentation. In the new framework, we classify pheromone into finite grades, the higher the grade, the more the pheromone. If an arc belongs to the best solution found so far, the grade of this arc would be increased, vice versa. Let $\tau_{\min}$ and $\tau_{\max}$ be the minimal and maximal pheromone trail, $h(i,j,k)$ be the grade of arc (i,j,k), $g(x)$ be a real positive increasing function , it maps grade to pheromone, let $g(1)=\tau_{\min}$ and $g(M)=\tau_{\max}$, r_1 is penalty number, r_2 is encouragement number, M is maximal grade, here r_1, r_2 and M are integers, $\hat{w}$ is the best feasible solution found so far, w_t is the best feasible solution found in current iteration, in our numerical calculations, we always fix $r_1=1$ and $\tau_{\min}=1$. Employing these symbols, we define the updating rules as follows:

(u8) $\forall(i,j,k)$: $h(i,j,k)\leftarrow h(i,j,k)-r_1$.

(u9) if $f(\hat{w})>f(w_t)$, then $\hat{w}=w_t$.

(u10) for $\hat{w}$, $\forall(i,j,k)\in\hat{w}$, $h(i,j,k)\leftarrow h(i,j,k)+r_2$.

(u11) $\forall(i,j,k)$: $h(i,j,k)\leftarrow\max(1,h(i,j,k))$.

(u12) $\forall(i,j,k)$: $h(i,j,k)\leftarrow\min(M,h(i,j,k))$.

(u13) $\forall(i,j,k)$: $\tau(i,j,k)=g(h(i,j,k))$.

where $\max(\bullet,\bullet)$ is maximum function, $\min(\bullet,\bullet)$ is minimum function.

For each ant, the transition probability from node i to j obeys solution construction rules

$$\mathrm{P}_{ij}=\begin{cases}\dfrac{\tau_{ij}^{\alpha}\cdot\eta_{ij}^{\beta}}{\sum_{r\in C_i}\tau_{ir}^{\alpha}\cdot\eta_{ir}^{\beta}}, & if \quad j\in C_i\\ 0, & otherwise\end{cases} \tag{18}$$

where C_i is the set of nodes that can be selected from node i, τ_{ir} is the pheromone of arc (i,r), η_{ir} is heuristic information of arc (i,r), α and β are parameters. And we choose

$$g(x)=\sqrt[m]{\frac{\tau_{\max}^{\ m}-1}{M-1}(x-1)+1}\ ,\ 1\le m \tag{19}$$

If $m=1$, $g(x)$ is a linear function, it changes equally, if $m>1$, $g(x)$ is a concave function, it changes fast at the beginning, and slowly later. Without speaking, we always let $m=2$.

FGACO uses maximal grade, encouragement number, penalty number and $g(x)$ to control the changing of pheromone. FGACO has three main features as follows:

1. The differentia between FGACO and standard ACO mainly lies in the rules of pheromone updating.
2. It classifies pheromone into finite grades, and pheromone updating is realized by changing the grades.
3. The updated quantity of a pheromone is independent of the objective function value, and the grade is changed by addition and subtraction operations.

3.2 Convergence analysis

In this subsection, FGACO is described as a finite Markov chain based on the properties of Markov chain. It will be shown that FGACO converges with probability 1 to the global optimum. The reader could see (Xu & Prince, 1998) for more details about Markov chains. An important property of finite Markov chains is given in the Lemma below (Xu & Prince, 1998).

Lemma 1

In any finite Markov chain, no matter where the process starts, the probability after *n* steps, that the process is in an ergodic state, tends to 1 as *n* tends to infinity.

The iterative process of FGACO is a discrete stochastic process. The states of this process are $s_n=(\tau(n),w(n))(n=1,2,...)$, all the states form the state space S, where $\tau(n)$ is the matrix of the pheromone values at the n^{th} cycle, $w(n)$ is the best solution found so far until the n^{th} cycle is a discrete vector. s_n can only take one of the finite values, therefore S has finite states.

On account of the solution construction rules, we have Proposition 1 for FGACO, S is a finite Markov chain. Due to the pheromone updating rules (u8), (u9) and (u10), we have Proposition 2 for FGACO, if $s_n, s_m \in S$, let $P_{s_n s_m}$ be the transitive probability from s_n to s_m, $P_{s_n s_m}$ has following results:

- if $f(H(s_n))<f(H(s_m))$, then $P_{s_n s_m}=0$
- if $H(s_n)=H(s_m)$, and exist the arc $(i,j)\in H(s_n)$, $G_{(i,j)}(s_n)>G_{(i,j)}(s_m)$, then $P_{s_n s_m}=0$

where $f(\bullet)$ is the objective function, here, we only discuss minimal optimization problem, $H(\bullet)$ is the vector function, it maps state space into feasible solution space, $G_{(i,j)}(\bullet)$ is the real function, it maps the state space into grade, here (i,j) is the arc. Therefore, two cases will occur if the state changes, the one is that the best solution, found so far changes, and the objective function value decreases, the other is that the objective function value holds the same, and the pheromone of arcs corresponding to the best solution increases. For the latter case, on account of (u1) and (u3), the pheromone of all the arcs converges after finite cycles, all the pheromone keeps changeless and the pheromone of the arcs corresponding to the best solution is $\tau_{\max}$, the pheromone of the other arcs is 1. The state space can be partitioned into three sorts.

Definition 1 (stagnant state, optimal state and normal state)

For $s\in S$, pheromone of the arcs corresponding to the best solution is $\tau_{\max}$, the pheromone of the other arcs is 1, then s is called a stagnant state. Furthermore, if $H(s)$ is the global

optimal solution, then s is an optimal state. The other states are called normal states. For an optimal state s^*, due to (u8), (u9) and (u10), we know that $P_{s^*s^*} = 1$, so an optimal state is an absorbing state. Based on Proposition 2 and the definition of transient state, it is convenient to show that the other states are transient states.

Theorem 1

For FGACO, $s_n = (\tau(n), w(n))$ is the finite Markov chain, every state is either transient or absorbing and all optimal states are absorbing states. As a result of theorem above, we have the following convergent property of FGACO.

Theorem 2

For FGACO, the probability of finding optimal solutions at least once is one as the cycle n tends to infinite.

3.3 FGACO for image segmentation

3.3.1 Energy function

For convenience, in Eq. (10), the external energy $E_{ext}(v)$ is defined in Eq. (20)

$$\int E_{ext}(v)ds = -\gamma \int \left\| f(\nabla I) \right\|^2 ds \tag{20}$$

In discrete form, $E_{ext}(v)$ can be defined as

$$E_{ext}(i) = -\gamma \left| f(g_i) \right|^2 \tag{21}$$

where g_i , the normalized value of the gradient $\nabla I(v_i)$ is expressed in Eq. (22)

$$g_i = \frac{\nabla I(v_i)}{g_{\max}} \tag{22}$$

where $g_{\max}$ is the maximum gradient on the individual search grids.

A nonlinear mapping function is incorporated to transform the normalized gradient so that it discourages the contour to adhere to low gradient region (Mishraa et al., 2003).

$$f(g_i) = \frac{1}{1 + \exp(0.7 - c \times g_i)} \tag{23}$$

Therefore, the final energy function of Eq. (10) can be written in the form

$$E_{snake} = \sum_{i=0}^{n-1} (\omega_1 \left| v_i - v_{i-1} \right|^2 + \omega_2 \left| v_{i-1} - 2v_i + v_{i+1} \right|^2) / 2 - \omega_3 \left| f(g_i) \right|^2 \tag{24}$$

where ω_1 , ω_2 , ω_3 are assumed to be constants over the whole boundary. The boundary is detected by minimizing the energy function defined in Eq. (24).

3.3.2 Algorithm for image segmentation

The algorithm is described as follows:

Step 1. Given: Initial value $\forall(i, j, k)$, $\tau_{ijk} = \tau_0$, $\tau_0 \geq 0$; path t (decided by the initial contour).

Step 2. Calculate: For each dimension of search space, for each ant, select the next position v_{i+1}^{p} according to equation (18), until it satisfies the termination-criterion.
Step 3. Calculate: Energy E_{snake} of every path the ant passed, according to equation (20).
Step 4. Calculate: The minimized energy path $\hat{t}$ and update τ according to equation (u(8)~u(13)).
Step 5. Restoring: $\hat{t}$ is the best path of search space, so the best segmentation is obtained.

4. Experimental results

In order to illustrate our proposed algorithms, we have done two experiments separately for ACM based ACO and FGACO. They are in the same experimental environment.

4.1 Simulation and analysis for ACM based ACO

Taking the segment of the heart image and left ventricle (LV) as examples to illustrate the resolving process of ACO. The result is compared with other algorithms in the end.

4.1.1 Image preprocessing

In most of the cases, the initial solution to the contour detection algorithm in medical ultra sound transducers images is provided by manually outlined contours. However, we have implanted a preprocessing technique (Mishraa et al., 2003), such as, Gaussian and morphological, to detect an initial boundary followed by our ACO optimization procedure. A potentially good image is selected as Fig. 2(a), which is filtered by convolving with a 3 × 3 Gaussian low pass filter with variance σ = 3. To eliminate the noise in the image, two successive stages of morphological filtration, i.e., dilation and erosion have been applied. The rough initial contour is extract as Fig. 2(b).

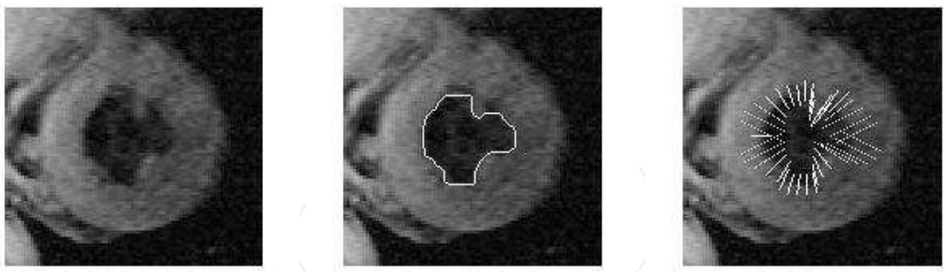

(a) (b) (c)

Fig. 2. (a) Origin picture of heart. (b) Initial contour of heart image. (c) Search space.

4.1.2 Construction of search space

From Fig. 2(b), we find the initial contour is a closed-ring. In order to apply the algorithm proposed above, the search space is constructed as follows:
Discretiaing the contour, we will get M differently equidistant points, those are P_i. Set the center of contour as C, a line is formed through C and P_i, so M lines are obtained, which is shown in Fig.2(c). We choose $2*N+1$ points along each line, of which P_i is the center. Get the average grey of every point in line section, the search space Ω is formed.

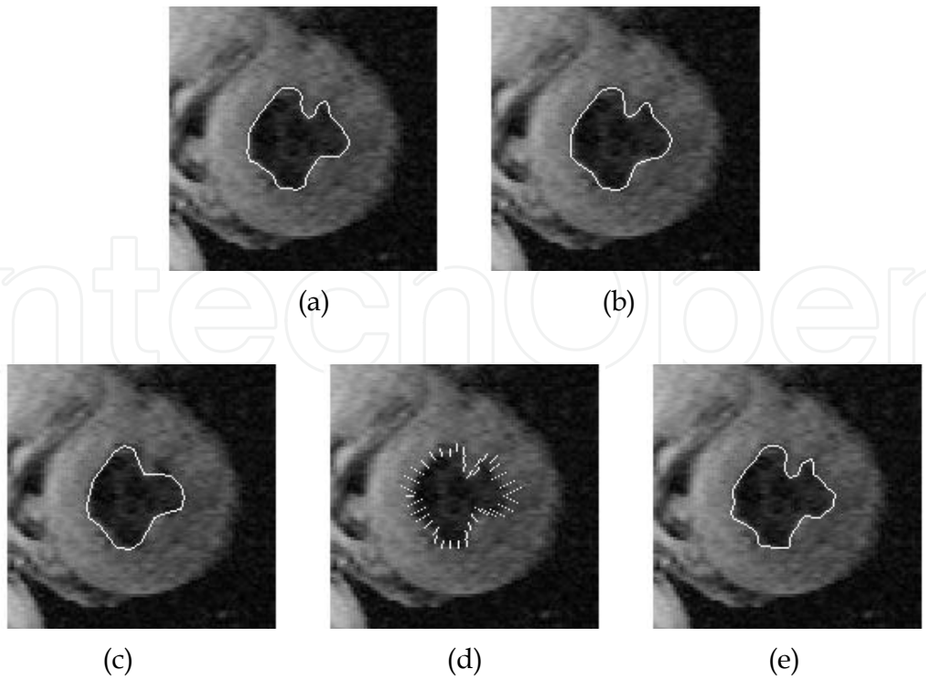

(a) (b)

(c) (d) (e)

Fig. 3. (a) Final contour. (b) Contour of the 2nd group of parameters. (c) Contour of the 3rd group of parameters. (d) Search space construction of N = 5. (e) Contour of N = 5.

4.1.3 Experimental results

Set parameters $N = 11, M = 100, A = 10$ (10 ants), the value w_1, w_2, w_3 refer to the 1st line in Table 1. And we always firmly use these parameters in our experiments unless we explain. The final result is shown in Fig. 3(a). It is obvious that the contour is more rational than that in Fig. 2(b).

Keep the parameters N, M, A unchangeable. The results of parameters of the 2nd and the 3rd group in Table 1 are illustrated in Fig. 3(b) and Fig. 3(c).

When the search space is shrunk, that is, N = 5, shown in Fig.3(d), the energy no longer decreases after 28 iterations, and the contour is displayed in Fig. 3(e).

Parameters / Energy*	ω_1	ω_2	ω_3	Iterations
13.0663	0.06	0.03	1	44
1.0309	0.6	0.6	0.1	50
72.6886	0.01	0.01	10	47

The mark * denotes the average of 10 times tests.

Table 1. Three groups of parameters and their results.

Furthermore, we test the performance with left ventricle shown in Fig. 4(a). The construction of search space is the same as what mentioned above. The initial contour is shown in Fig. 4(b), the final result with the parameters in 1st line in Table 1 is displayed in Fig. 4(c). The energy no longer decreases after 48 iterations.

(a) (b) (c)

Fig. 4. (a) left ventricle. (b) Initial Contour of LV. (c) Result with 48 iterations.

4.2 Experiment and analysis for FGACO

Here, we use the same example images of the heart image and left ventricle (LV) in Sect. 4.1. The method of preprocessing and construction of search space is the same as general ACO. Firstly, the boundary detection of heart image provides the detail process of FGACO image segmentation algorithm. Experiments with different parameters are done for performance evaluation. Secondly, we compare the results of FGACO with general ACO and GA with left ventricle (Mishraa et al., 2003).

4.2.1 Experimental results and performance evaluation with the heart image

Set $N = 11$, $M = 100$, $A = 10$ (10 ants), $a = 100$, $\tau_{\max} = 50$, $r_2 = 3$, the value ω_1, ω_2, ω_3 refer to the 1st line in Table 1. The final result is shown in Fig. 5(a). We can easily find that the contour is more rational than that in Fig. 2(b). Fix N, M, A, the results of parameters of the second and the third group in Table 1 are illustrated in Figs. 5(b) and 5(c).

To test the influence of the parameters maximal grade and the maximal pheromone value $\tau_{\max}$ on the optimization results, we set $N = 11$, $M = 100$, $A = 10$, $r_2 = 3$ and take the parameters ω_1, ω_2, ω_3 referring to the first line in Table 1. The compared results, with the difference a, is shown in Table 2. The compared results, with the difference $\tau_{\max}$, is shown in Table 3. From Table 2, we can see that if take the maximal grade a with small value $(a = 10)$, the algorithm reaches a premature solution with fewer iterations, while if take large value $(a = 100)$, the algorithm is with more iterations. The compared results of Table 3 suggest that the $\tau_{\max}$ should be limited in a suitable region.

Maximal grade a	10	50	100	1000
Energy*	14.067	12.0663	12.0663	12.0663
Iteration Number*	18	20	24	42

Table 2. Influence of parameter maximal grade a with $\tau_{\max} = 50$.

Maximal pheromone $\tau_{\max}$	10	50	100	1000
Energy*	18.067	12.0663	12.0663	24.0663

Table 3. Influence of parameter maximal pheromone $\tau_{\max}$ with $a = 100$.

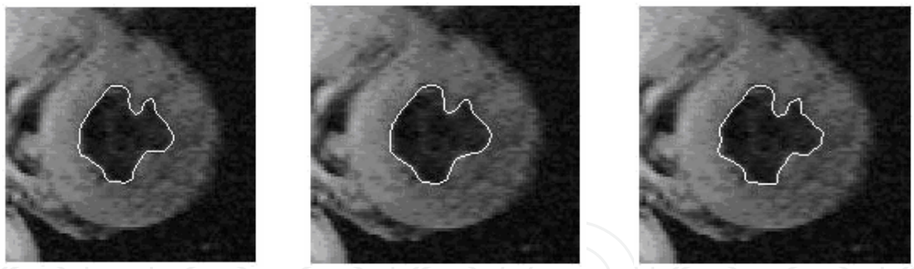

(a) (b) (c)

Fig. 5. (a) Optimized contour with the first parameters in Table 1. (b) Optimized contour with the second parameters in Table 1. (c) Optimized contour with the third parameters in Table 1.

4.2.2 Compared results with general ACO and GA for left ventricle

In order to compare FGACO algorithm with others and test the influence of the new finite grade pheromone updating rule on optimization process, we select the boundary detection of left ventricle which is also considered in literature (Mishraa et al., 2003). A potentially good left ventricle image is selected as Fig. 6(a). We take the same preprocessing in Sect.4.1.1, and obtain the initial contour as Fig. 6(b). The construction of a search space is the same as in Sect. 4.1.2. Firstly, we detect the boundary with a general ACO, the result of which is shown as Fig. 6(d). The result with FGACO is shown in Fig. 6(e). Conveniently, we place the segment results by GA of (Mishraa et al., 2003) in Fig. 6(f). Also, the fitness curves by iterations (or generations) are showed in Fig. 8.

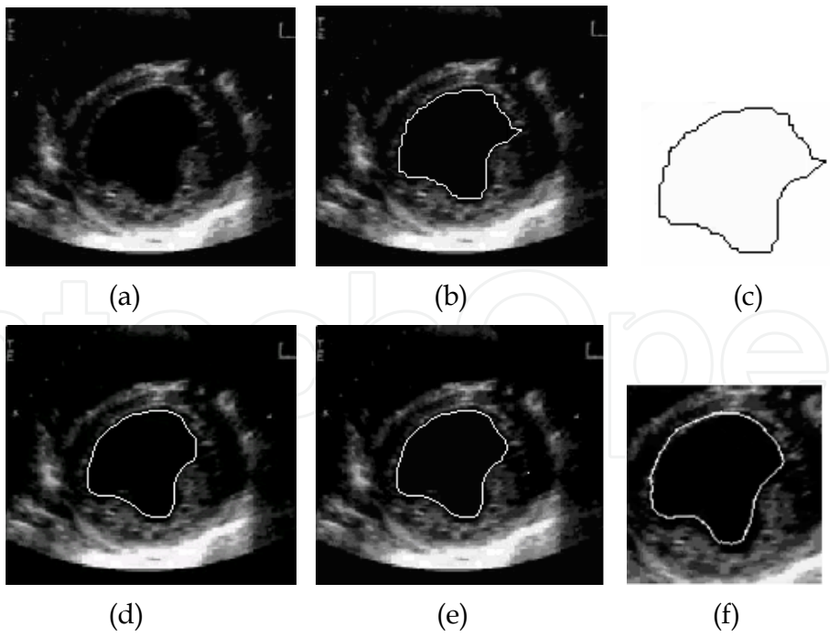

(a) (b) (c)

(d) (e) (f)

Fig. 6. (a) Original ultrasound image of left ventricle. (b) Rough boundary of the endocardial boarder on original image. (c) Rough boundary of the endocardial boarder on original image. (d)Optimized contour by general ACO. (e) Optimized contour by FGACO. (f) Optimized contour by GA of reference (Mishraa et al., 2003).

By observing the images from Figs. 6(d) to 6(f), it is obvious that the three optimization algorithms can successfully extract the boundary. But ACO based algorithms detect with fine boundary and FGACO algorithm is more effective. Furthermore, the extracted boundaries agree with the human visual judgment and are exactly consistent with the true ones in the original grey level images. From Fig. 7, we can note that the computational times required for each generation are different for different algorithms. Evidently, in our experiment, the computing efficiency of the FGACO is the best which shows the effectiveness of finite grade pheromone updating rules.

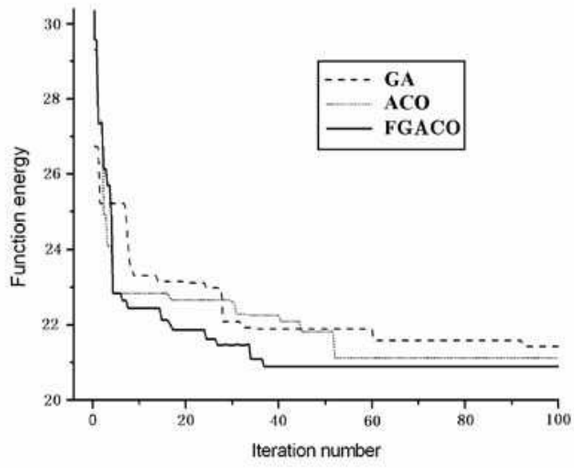

Fig. 7. Function energy comparison of FGACO with ACO and GA

5. Algorithm in phase change line detection of thermography

5.1 Phase change thermography sequence

During the research and development of aerocraft, we always need to obtain the heat distribution on the aerocraft surface. The phase change thermography is a test technique in wind tunnel for measuring thermal flow in a large area(Tang & Huang, 2003; Zhang & Fang, 1995), which becomes an effective way to get the thermography map. Theoretically, the color of the phase change material will change with a given temperature of the test object from white to black, which gradually form the boundary between two parts on the surface, called phase change line(PCL) (Tang & Huang, 2003). The key of this technique is to extract the PCL from phase change thermography sequence (PCTS). However, owing to the bad condition in wind tunnel and the complexity of aero-craft surface, sequence images are noisy(see in Fig. 8), which contributes to the difficulty of sequence image analysis, and that's why common segmentation methods does not work well. Fig. 8 gives out some frames in PCTS, and in order to clearly capture the phase change process, we install lights in the corner of the room, which leads to reflection on the surface, as showed in Fig. 8(d).

In order to address problems mentioned above, a new dynamic programming method has been proposed by Wang et al., which works well on the models with simple surface. In his method, the initial PCTS is transformed into a series of synthesized images by compression and conversion, then, a virtual illumination model is formulated to eliminate the influence of specular reflection, and finally, the approving isotherm is gained after the glisten is

removed (Wang & Feng, 2007). Here, we replace the dynamic programming method described above by our ACO algorithm. We first divide PCTS into multiple associated sub-images, then, we use ACO algorithm to extract PCL for each sub-image, so finally we can obtain the target PCL after combining all the sub-image PCLs.

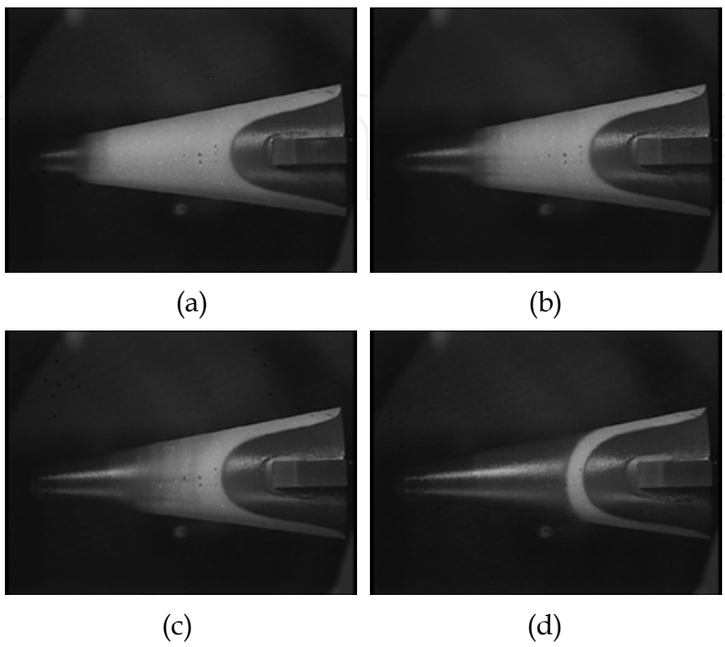

Fig. 8. Some frames in PCTS. (a) the 96th frame. (b) the 180th frame. (c) the 237th frame. (d) the 364th frame.

5.2 Ant colony optimization for phase change line detection

5.2.1 Image segmentation algorithm for PCTS

From Fig. 8, we can see that PCL is a fuzzy band so that it is difficult to segment every frame individually using traditional methods. Therefore, using the information of target motion and solving the image segmentation problem concerning the whole sequence is a quite large challenge. We propose an image segmentation algorithm for PCTS based on region-division, and we will realize image segmentation under ACO. The process of segmentation is showed in Fig.9.

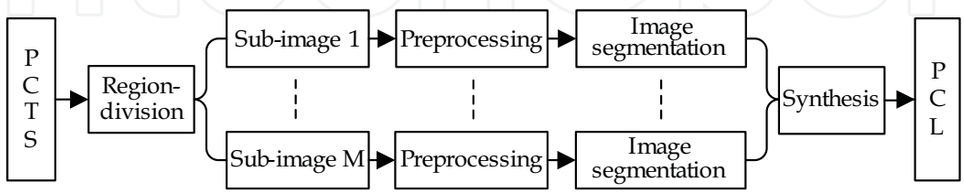

Fig. 9. Segmentation process in PCTS

5.2.1.1 Region-division

Sequence image can be expressed as $\Phi = \{\psi_1(x,y), \psi_2(x,y), \cdots, \psi_N(x,y)\}$, where $\psi_i(x,y)$, (x,y) is the image coordinate, and $i = 1,2,\cdots,N$ is one domain in image sequence, also be

called frame. Each frame $\psi_i(x,y)$ is divided into M sub-regions $\psi_{ij}(j=1,2,\cdots,M)$ and a background sub-region ψ_{ib}, that is, $\psi_i=\sum_{j=1}^{M}\psi_{ij}+\psi_{ib}$. Here the sub-regions and the back ground satisfy $\psi_{iS}\cap\psi_{ij}=\phi(s\neq j)$, $\psi_{ib}\cap\psi_{ij}=\phi(j=1,2,\cdots,M)$, separately. Therefore, we divide image sequence Φ into M sub-sequence, namely, $\Phi_j=\{\psi_{1j},\psi_{2j},\cdots,\psi_{Nj}\}$, $j=1,\cdots,M$. Based on the characteristics of PCTS, we can easily separate the object region from background. To take advantage of the correlation among image sequence, we split each segmented object into M sub-regions. The split steps are as follows:

1. Separate the needed region from target image.
2. Divide the left part of needed region into M copies, and so does the right part.
3. Each frame forms M sub-regions.

Fig.10 shows the division results of some region in a PCTS example, where $M=9$.

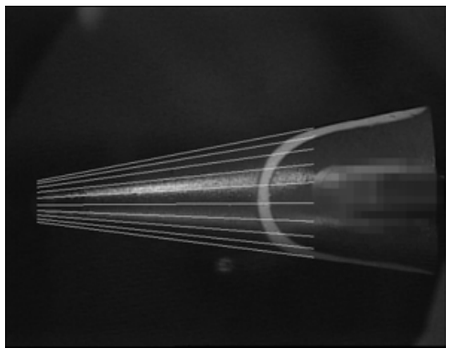

Fig.10. An example of region-division $(M=9)$

5.2.1.2 Region-space conversion

For each sub-region ψ_{ij}, we take the longitudinal axis as main direction, compute the sum of grey value of all pixels, and then divide it by the number of pixels, i.e.

$$c(j,k)=\frac{1}{n_k}\sum_{s=y_k}^{y_k+n_k}\psi_{ij}(k,s),\ i=1,\cdots,N;j=1,\cdots,M \tag{25}$$

where n_k is the number of pixels on the horizontal axis k in sub-sequence image, $\psi_{ij}(k,s)$ represents the grey value of j th region coordinate (k,s) in i th image, y_k is the minimum vertical axis on the horizontal axis k in sub-sequence image, and $k=1,2,\cdots,H$ is the length of image domain.

In this way, each original phase-change image is transformed into a $M\times H$ grey scale matrix. Thus, the whole image sequence is transformed into N matrixs with $M\times H$. Take the same line of each matrix in turn, so the whole image sequence Φ comes into being M images with $N\times H$. Fig. 11 shows the conversion process where $M=9,N=600,H=500$ and conversion results are given out in Fig. 12. From Fig. 12, it is apparent that we have transformed the original PCTS to M segmented images. Here, the transformed image is called sub-image, and then we will introduce the segmentation of sub-image.

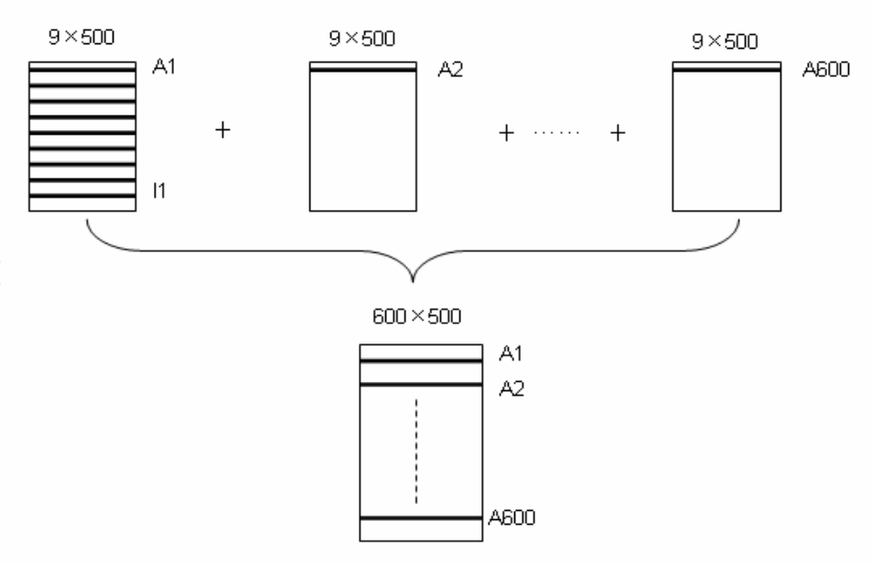

Fig. 11. Conversion process

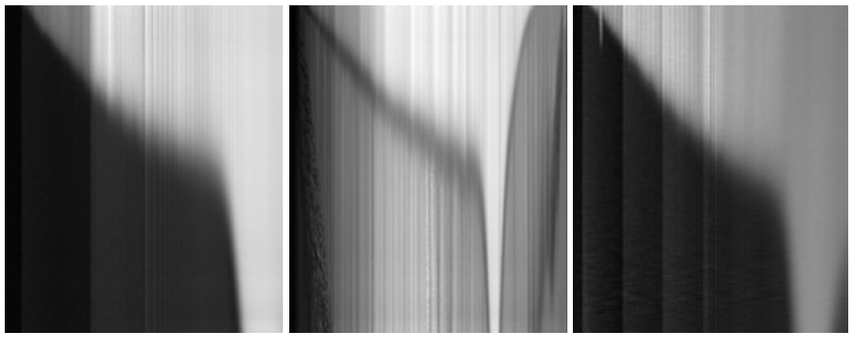

1st 4th 9th

Fig. 12. Some sub-images

5.2.1.3 The preprocessing of sub-image

From Fig.12, we can see that the sub-images are noisy because of the illumination and reflection . The preprocessing including three steps is performed to improve the sub-image. First, smoothing technique is used to eliminate image noise with a mean filter. Second, in order to eliminate the influence of specular reflection, we do the following processing for image data in each column: if $f(i,j) > f(i,j-1)$, then $f(i,j) = f(i,j-1)$. Third, a normalizeation step is carried out with the image from left to right in each column, that is, for every pixel (m,n) in a given image $f(i,j)$, the grey value is calculated according to

$$f'(i,j) = \frac{f(i,j) - f_i^{\min}}{f_i^{\max} - f_i^{\min}} \tag{26}$$

where $f_i^{\min}$ and $f_i^{\max}$ is the minimum and maximum grey value in i th column, separately.

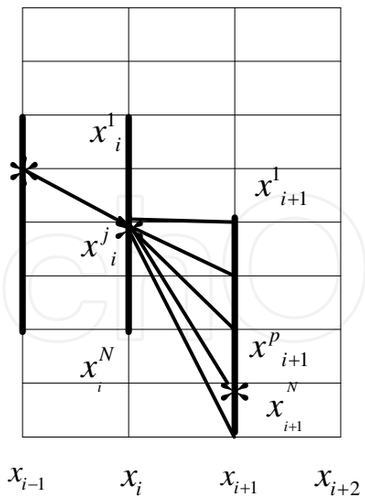

Fig. 13. Example of search

5.2.2 ACM based ACO image segmentation algorithm

ACM based ACO image segmentation algorithm has already been proposed in Sect.2. Here, we will apply the algorithm to realize the sub-image segmentation.

5.2.2.1 Construction of search space

After the normalization, we must choose an initial segmentation line in order to construct the search space of our ACO algorithm. The detail is stated as follows:

Step 1. Draw a grey value changes curve from left to right under a column unit and determine the upper edge and lower edge of the grey value, respectively denoted as MAX and MIN.

Step 2. For MAX and MIN in every column, we do: $mean = \alpha \cdot MAX + (1-\alpha) \cdot MIN$, where α is the coefficient to be determined.

Step 3. In terms of the grey value changes curve, the pixel value of middle point corresponds to its vertical axis. Therefore, for each $mean$ in every column, we can find a point corresponds to it until every point is determined. These points form an initial segmentation line, according to which we draw a segmentation band with bandwidth δ.

From the phase change process, we know that the PCL in present image must have shifted back from the previous one, that is, the present coordinate value of segmentation line is greater than the previous one(coordinate value is shown in Fig. 13). We suppose the present coordinate value is x_i^j, so the feasible zone of next point is $\vartheta = \{x_{i+1}^k \mid j \le k \le j+\delta \,\&\, k \in \Psi\}$, where δ is the search space given out.

5.2.2.2 Algorithm description

The energy function is defined as:

$$E_{snake} = \sum_{i=1}^{n} \{\alpha[|x_i - x_{i-1}| + |y_i - y_{i-1}|] + \beta[|x_{i-1} - 2x_i + x_{i+1}| + |y_{i-1} - 2y_i + y_{i+1}|] + wf(\nabla I)\} \quad (26)$$

where x_i, y_i is the coordinate value of present segmentation line, $f(\nabla I)$ is the edge energy in image force, and ∇I represents the first order difference of grey value I. α, β, w are the coefficients given out.

The target of our algorithm is to find an optimal path t^* in search space Ψ, which contributes to the minimum of energy function. Our algorithm includes definition of pheromone, probability decision, and pheromone update, which have already been introduced in Sect.2.3. Furthermore, the description of our algorithm is the same as Sect.2.3.4.

5.2.2.3 Segmentation results

Set $N = 10, M = 60, A = 10, \alpha = 5, \beta = 0.1, w = 2$ and the final results is shown in Fig. 14.

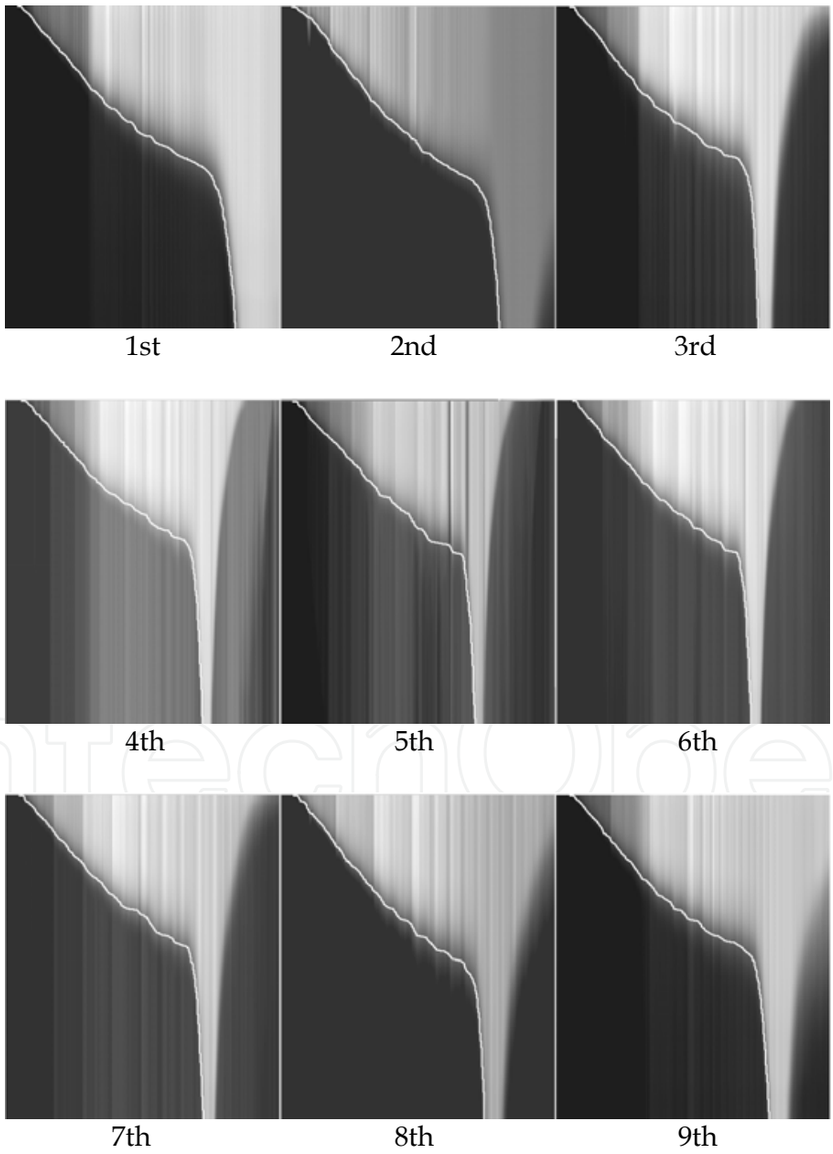

Fig. 14. Results of sub-image segmentation

After obtaining the PCL of sub-image, we can return it to original image sequence. As we divide the segmented object into *M* sub-regions, the points that return from PCL to original image sequence locate in the middle of *M* sub-regions. Then we use quadratic spline to fit these points so that we acquire the final PCL, shown in Fig. 15.

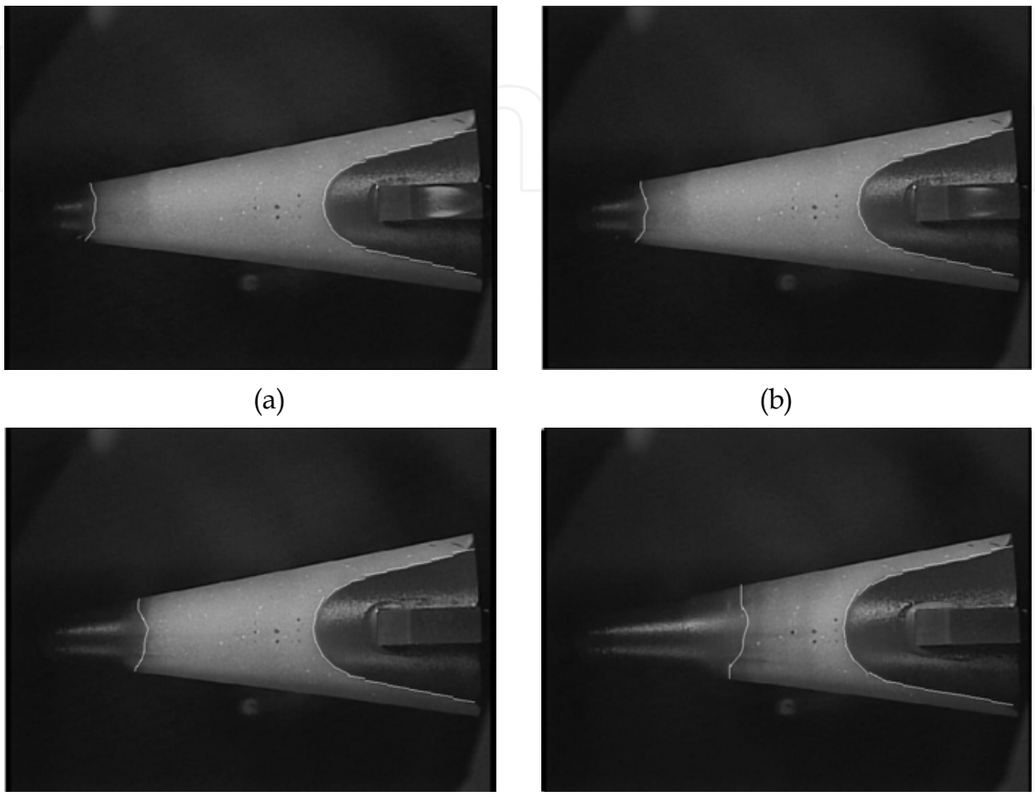

(a) (b)

(c) (d)

Fig. 15. Some results of PCTS segmentation. (a) 100th frame (b) 120th frame (c) 180th frame (d) 284th frame

6. Discussion and conclusion

This chapter describes application of the ACO algorithm to the image segmentation problems. First, based on the similarity between the solving process of ACM and ACO, the ACO algorithm for image segmentation is proposed. Taking medical image segmentation as examples, the result indicates that the contour is continuous, and more smooth and rational than the raw contour (shown in Figs. 3,4). This algorithm provides a new approach to obtain precise contour. It is proved to be convergent with probability one, and will reach the best feasible boundary with minimum energy function value. Moreover, this algorithm can also be used to solve other revised ACM problems.

In addition, a new pheromone updating rule is designed for improving the time performance of the algorithm. The convergence prosperities are given by finite Markov chain. The proposed algorithm has been tested for automatic boundary detection of the endocardial border in a set of ecdocardio graphic images.

Finally, we have introduced the application of the proposed algorithm in phase change line detection of complex phase change thermography. In the algorithm, phase change sequence is changed into multiple associated sub-images by region division which includes the moving information of the moving contour.

The main contribution of this paper is to apply ACO in optimum contour extraction for noisy images. Even though implementation of ACO in discrete combinational optimization problems is successful, the results of the general ACO found to be time-consuming because feasible decision set increases exponentially with the dimension of the decision variable. By introducing the finite grade pheromone updating rules, the contour extraction is reasonably insensitive to the initial approximation in the search space. The experimental results show that our general ACO algorithm for image segmentation is more effective than the genetic algorithm in related literature, and our FGACO algorithm works quite satisfactorily, and ultimately reduces computational time compared to general ACO (shown in Figs. 6,7).

The experimental results with the PCTS show that the algorithm extracts the phase change active contour well. But as the relationship between multi-regions is not taken into account by us, the segmentation results cannot reach perfect accuracy. Therefore, our future work will focus on how to use the coordinate characteristics between the individuals of ant colony to solve the problem mentioned above.

7. Acknowledgements

This work is partially supported by the Natural Science Foundation Fund of China Grant #60475023 and the Natural Science Fundation Fund of Zhejiang Province Grant #Y106660. In addition, we are also thankful to Liangjun Ke, Zuren Feng from Xi'an Jiaotong University for their stimulating comments and useful supports, which helped to improve the quality of the manuscript.

8. References

Kass, M.; Witkin, A. & TeizoPoulos, D. (1987). Snakes: active contour models[J]. *International Journal of Computer Vision*, 1(4): 321 - 331

Cohen, L.D. (1991).On active contour models and balloons, *Computer Vision Graph.* 53, 211–218.

Amini, A.A.; Weymouth T.E. & Jain, C.R. (1990). Using dynamic programming for solving variational problems in vision, *IEEE T. Pattern Anal.* 12, 855–867.

Williams, D.J. & Shah M. (1990). A fast algorithm for active contours, *Proc. 3rd Int. Conf. on Computer Vision*, 592–595.

MacEachern, L.A. & Manku, T. (1998). Genetic algorithms for active contour optimization, *Proceedings - IEEE International Symposium on Circuits and Systems* 4, 229–232.

Gunn, S.R. & Nixon, M.S. (1996). Snake head boundary extraction using global and local energy minimization, *Proc. 13th Int. Conf. on Pattern Recognition*, 581–585.

Xu, C. & Prince, J.L. (1998). Snake shape and gradient vector flow, *IEEE T. Pattern Anal.* 7, 359–369.

Hsien-Hsun, W.; Jyh-Charn, L. & Chui, C. (2000). A wavelet-frame based image force model for active contouring algorithms, *IEEE T. Image Process.* 9, 1983–1988.

Lam, K.M. & Yan, H(1994). Fast greedy algorithm for active contours, *Electronics Letters*, v 30, p 21-23.

Dorigo, M; Manjezzo, V. & Colorni, A. (1996). The ant system: Optimization by a colony of cooperating agents. *IEEE Transaction on Systems, Man& Cybernetics B*, 2692: 29-41.

Dorigo, M. & Ganbardella, L.M. (1997). Ant colony system: A cooperating learning approach to the traveling salesman problem. *IEEE Transactions on Evolutionary* Computation. 1997, 1(1), 53-66.

Bullnheimer, B.; Hartl, R. & Strauss, C. (1998). Applying the ant system to the vehicle routing problem. Meta-Heuristics: Advances and Trends in Local Search Paradigms for Optimization [M], *Kluwer Academics*, pp. 285-296.

Stutzle, T. (1998) An ant approach to the flow shop problem[C]. *Proceedings of European Congress on Intelligent Techniques and Soft Computing*. Aachen, Germany, 1560-1564.

Ouadfel, S. & Batouche, M. (2003). Ant colony system with local search for Markov random field image segmentation [C], *International Conference on Image Processing*, 1:133-136

Meshoul, S. & Batouche, M. (2002). Ant colony system with external dynamics for point matching and pose estimation [J]. *Pattern Recognition*, 2002. 3 :823 – 826.

Feng, Y.J. (2005). Ant colony cooperative optimization and Its Application in image segmentation. Dissertation of Ph.D. Xi'an Jiaotong University. China.

Han, Y. F. & Shi, P. F. (2006). An improved ant colony algorithm for fuzzy clustering in image segmentation. *Neurocomputing,* 70 (2007) 665-671.

Tao, W.B.; Jin, H. & Liu, L.M. (2007). Object segmentation using ant colony optimization algorithm and fuzzy entropy. *Pattern Recognition Letters* 28 788-796.

Hegarat-Mascle, L.; Kallel, S. & Velizy, A. etc. (2007). Ant Colony Optimization for image regularization based on a nonstationary markov modeling, *IEEE Transactions on Image Processing*, 16(3): 865-878.

Ma, L.; Wang, K.Q. & Zhang, D. (2009). A universal texture segmentation and representation scheme based on ant colony optimization for iris image processing. *Computers and Mathematics with Applications* 57 (2009) 1862_1868.

Susmita, G.; Megha, K.; Anindya, H. & Ashish, G. (2009). Use of aggregation pheromone density for image segmentation. *Pattern Recognition Letters* 30 (2009) 939-949.

Lao, D.Z. (2004) Foundation of variational methods. *National Defense Industry Press*. p.85-88

Mishraa, A.; Duttab, P.K. & Ghoshc, M.K. (2003). A GA based approach for boundary detection of left ventricle with echocardio graphic image sequences. *Image and Vision Computing* 21 (2003) 967–976.

Tang, Q. & Huang, G. (2003). The reaserch and application of phase change thermograghy technique, *Experiments and Measurements in Fluid Mechanics*, 17(1):15-17(in Chinese).

Zhang, J. & Fang, D. (1995). The application of the phase change thermo-graghy technology in measurement of surface heat transfer rate, *Aerodynamic Experiment and Measurement Control*, 1995, 9(1):67-72(in Chinese).

Wang, X. & Feng, Z. (2007). The automatic extraction of isothermal line in phase-change thermograthy sequence, *Pattern Recognition and Artificial Intelligence*, 20(4):469-477(in Chinese).

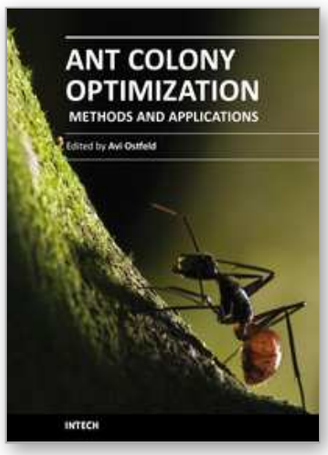

Ant Colony Optimization - Methods and Applications

Edited by Avi Ostfeld

ISBN 978-953-307-157-2
Hard cover, 342 pages
Publisher InTech
Published online 04, February, 2011
Published in print edition February, 2011

Ants communicate information by leaving pheromone tracks. A moving ant leaves, in varying quantities, some pheromone on the ground to mark its way. While an isolated ant moves essentially at random, an ant encountering a previously laid trail is able to detect it and decide with high probability to follow it, thus reinforcing the track with its own pheromone. The collective behavior that emerges is thus a positive feedback: where the more the ants following a track, the more attractive that track becomes for being followed; thus the probability with which an ant chooses a path increases with the number of ants that previously chose the same path. This elementary ant's behavior inspired the development of ant colony optimization by Marco Dorigo in 1992, constructing a meta-heuristic stochastic combinatorial computational methodology belonging to a family of related meta-heuristic methods such as simulated annealing, Tabu search and genetic algorithms. This book covers in twenty chapters state of the art methods and applications of utilizing ant colony optimization algorithms. New methods and theory such as multi colony ant algorithm based upon a new pheromone arithmetic crossover and a repulsive operator, new findings on ant colony convergence, and a diversity of engineering and science applications from transportation, water resources, electrical and computer science disciplines are presented.

InTech Europe
University Campus STeP Ri
Slavka Krautzeka 83/A
51000 Rijeka, Croatia
Phone: +385 (51) 770 447
Fax: +385 (51) 686 166
www.intechopen.com

InTech China
Unit 405, Office Block, Hotel Equatorial Shanghai
No.65, Yan An Road (West), Shanghai, 200040, China
中国上海市延安西路65号上海国际贵都大饭店办公楼405单元
Phone: +86-21-62489820
Fax: +86-21-62489821

IntechOpen